Topological regulation of activation barriers on fractal substrates

Raffaella Burioni
Dipartimento di Fisica e Scienza della Terra and INFN, Gruppo Collegato di Parma, Università di Parma, Parco Area delle Scienze 7/A, I-423100 Parma, Italy

Federico Corberi
Dipartimento di Fisica "E. R. Caianiello"; INFN, Gruppo Collegato di Salerno; and CNISM, Unità di Salerno, Università di Salerno, via Ponte don Melillo, 84084 Fisciano, Salerno, Italy

Alessandro Vezzani
Centro S3, CNR Istituto di Nanoscienze, Via Campi 213A, 41125 Modena, Italy and Dipartimento di Fisica Scienza della Terra, Università di Parma, Parco Area delle Scienze 7/A, I-43100 Parma, Italy

(Received 3 December 2012; published 25 March 2013)

We study the phase-ordering dynamics of a ferromagnetic system with a scalar order-parameter on fractal graphs. We propose a scaling approach, inspired by renormalization-group ideas, where a crossover between distinct dynamical behaviors is induced by the presence of a length λ associated with the topological properties of the graph. The transition between the early and the asymptotic stages is observed when the typical size $L(t)$ of the growing ordered domains reaches the crossover length λ. We consider two classes of inhomogeneous substrates with different activated processes, where the effects of the free-energy barriers can be analytically controlled during the evolution. On finitely ramified graphs, the free-energy barriers encountered by domains walls grow logarithmically with $L(t)$, whereas they increase as a power law on all other structures. This produces different asymptotic growth laws (power laws vs logarithmic) and a different dependence of the crossover length λ on the model parameters. Our theoretical picture agrees very well with extensive numerical simulations.

DOI: 10.1103/PhysRevE.87.032160 PACS number(s): 64.60.Cn, 05.70.Ln, 61.43.Hv, 05.50.+q

I. INTRODUCTION

The slow relaxation of glasses, spin glasses, and phase-separating systems is a subject of paramount importance in nonequilibrium statistical mechanics. In the case of homogeneous ferromagnets, i.e., nondisordered magnetic systems defined on homogenous substrates such as lattices, the basic features of the dynamics after a quench below the critical temperature are well understood in terms of the domain growth mechanism [1]. The unbounded growth of the size of ordered domains with nearly equilibrium composition involves a scaling symmetry due to the presence of a dominant length scale, which is manifested in the lack of time-translational invariance and aging. Although this simple paradigm of slow relaxation is expected to encompass a broad variety of situations, its applicability to more complex systems, such as spin glasses, where both homogeneity and ferromagnetism are spoiled, remains a debated issue [2]. An intermediate class of systems is that of nonhomogeneous ferromagnetic materials [3]. In these systems space homogeneity is wrecked by spacial modulations of some relevant parameter that, in order to maintain the system ferromagnetic, must coexist with the low-temperature order. In this case phase-ordering kinetics is preserved, although interesting new features may arise. The agent whereby homogeneity is spoiled may be random, such as random fields, random bonds, or dilution, or deterministic, as in the case of models defined on deterministic graphs. The kinetics of these systems has been an active area of research for quite some time now. A unifying feature is the ubiquitous appearance of energetic barriers slowing down the motion of domain boundaries. This happens because, due to space inhomogeneity, interfaces are pinned in particular positions, which may have dramatic consequences on the growth law and the properties of correlation functions [4–7]. Despite many experimental and theoretical studies [3], a number of issues are still open. In particular, the conditions under which inhomogeneities may radically modify the asymptotic dynamics are not *a priori* known [8]. Indeed, there are cases where disorder merely changes the time units, such as the one-dimensional Ising model with random bond [6], and others, such as the same model but with disorder in the form of a random field [9], where profound qualitative modifications occur. For this second class of systems the nature of both the dynamical scaling symmetry and the asymptotic growth law is not yet fully characterized. Related to that, the conjecture of a superuniversal behavior, namely, the idea that scaling functions are robust with respect to the presence on inhomogeneities that do not change the low-temperature properties of the system [10], has been proposed.

Recently, in the context of disordered ferromagnets, the observed behavior has been interpreted [11] in terms of a picture inspired by renormalization-group ideas where disorder introduces, in addition to the domain size, another characteristic length that gives rise to a crossover pattern. In this paper we apply similar ideas to the realm of ferromagnets defined on nonhomogeneous physical [12] fractal graphs, which turn out to be a simple but paradigmatic case where energy barriers thoroughly modify the asymptotic behavior of phase-ordering dynamics. Indeed, at variance with the case of disordered systems, the nature of the energetic barriers and their scaling properties can be reasonably well understood and can be related to the topological inhomogeneity. This allows one to make precise predictions about the growth laws, the scaling properties, and the crossover phenomena. These

 ©2013 American Physical Society

predictions conform quite well to the outcome of numerical simulations of the dynamics of the Ising model on graphs. The main result of this paper is the existence of a crossover from an early power-law behavior to a slower asymptotic growth. The latter may be a power law (with a smaller temperature-dependent exponent) or logarithmic according to the structure of the barriers, which in turn depends on the topology of the graph. In particular, we conjecture power laws to be associated with graphs that sustain ferromagnetic order only at zero temperature, while logarithms are expected if an ordered phase exists. The scaling functions of correlation functions are sensitive to the crossover.

This paper is organized as follows. In Sec. II we provide an overview of domain growth laws and the scaling framework proposed in Ref. [11] for disordered systems. In Sec. III we specify and adapt the scenario to the case of ferromagnets on graphs, providing also predictions for several quantities such as crossover lengths and exponents. In Sec. IV we present numerical results for the phase ordering of the Ising model on three model fractal graphs: the Sierpinski carpet (SC), the Sierpinski gasket (SG), and the T fractal (TF). For the first structure a low-temperature ordered phase exists, whereas it is not sustained in the other two. We will argue this fact to represent a basic difference for the dynamical evolution. The numerical results are interpreted using the scaling ideas of Secs. II and III and agree quite nicely with the predictions obtained there. In Sec. V we conclude with a summary and a discussion of the generality of our results.

II. GROWTH LAWS AND DYNAMICAL SCALINGS

Domain growth kinetics is characterized by an ever increasing typical domain size $L(t)$ after the quench of a system to a final temperature T in the ordered phase. When $L(t)$ becomes the dominant length in the problem, dynamical scaling is observed, meaning that all other lengths can be measured in units of $L(t)$. Such a property is reflected, for instance, in the two-point and two-time order parameter correlation function $\mathcal{G}(r;t,t_w)$, where r is the distance between the two points and $t > t_w$, which in homogeneous systems scales as [13]

$$\mathcal{G}(r;t,t_w) = \widehat{\mathcal{G}}[r/L(t), L(t_w)/L(t)], \tag{1}$$

$\widehat{\mathcal{G}}$ being a scaling function.

Generally speaking, the growth law and other properties such as $\widehat{\mathcal{G}}$ may depend on several factors, e.g., temperature, conservation laws, dimensionality, order parameter symmetry, disorder, and topology of the substrate. In the simplest cases, as in homogeneous magnets with nonconserved dynamics, the kinetics proceeds without activation events. This means that no free-energy barriers are encountered in the evolution and, consequently, phase ordering is observed down to temperature $T = 0$. In this case the typical domains size increases as $L(t) \sim t^{1/2}$. In contrast, the kinetics of other coarsening systems require thermal activation. The simplest example are perhaps homogeneous magnets with conserved dynamics. In this case energy barriers arise as due to the microscopic evaporation-condensation mechanism underlying the evolution [14]. In general, barriers can have different origin and scaling properties. In nonhomogeneous systems, such as the disordered ones or those embedded in a nonhomogeneous substrate, they are typically due to the pinning of interfaces in certain preferred positions. In a wide class of disordered systems, such as the Ising model with random fields [9,11,15,16], random bonds [17], or random dilution [7], this pinning effect asymptotically slows down the growth law to a logarithmic form

$$L(t) \propto [\ln(t/\tau)]^{1/\psi}, \tag{2}$$

where τ and ψ are model-dependent quantities. With an Arrhenius form

$$t \propto e^{\mathcal{E}/k_B T} \tag{3}$$

for the time needed to escape a barrier with activation free energy $\mathcal{E}$, the problem of establishing the growth law is directly related to the one of determining the typical height $\mathcal{E}$ of barriers at a certain stage of the evolution. Indeed, inverting the relation (3), one concludes that the typical activation increases with the domains size as a power law

$$\mathcal{E}(L) \propto L^{\psi}. \tag{4}$$

Equation (4) is not the only possible situation since a different algebraic growth law

$$L(t) \propto t^{1/\zeta}, \tag{5}$$

with ζ a temperature-dependent exponent, is observed asymptotically in systems defined on a class of fractal structures [18,19] and preasymptotically in random field [11] and random bond ferromagnets [4,5,17,20]. Plugging Eq. (5) into Eq. (3), one arrives at

$$\mathcal{E}(L) \propto [\ln(L)^{\zeta}] \tag{6}$$

for the scaling of the barriers with the domains size. A classification of phase-ordering systems according to the possible growth laws is made in Ref. [8]. In general, however, a complete characterization of $L(t)$ in the many varied instances of coarsening systems is lacking. Besides that, understanding the behavior of the scaling functions such as $\widehat{\mathcal{G}}$ in Eq. (1) is also an open problem.

In Ref. [11] it was proposed to unify the wide variety of behaviors observed in domain growth into a generalized scaling framework. The basic idea, originally conceived for disordered systems, is that the agent responsible for inhomogeneity introduces an extra characteristic length λ. In the case of the Ising model with nonconserved dynamics defined on a inhomogeneous graph considered in this paper (see Sec. III), the only parameters of the model are the ferromagnetic coupling constant J and T, which enter in the combination $\epsilon = J/T$. Then it must be that $\lambda = \lambda(\epsilon)$. The presence of λ introduces a crossover phenomenon between two different dynamical behaviors when $L(t)$ crosses λ. For the domain size this is assumed to be described by

$$L(t;\epsilon) = t^{1/z}\widehat{L}(\epsilon/t^{\phi}), \tag{7}$$

where z and ϕ are a growth and a crossover exponent, with a scaling function behaving as

$$\begin{aligned} &\widehat{L}(x) = \text{const} \quad \text{for } x \to 0 \\ &\widehat{L}(x) = x^{1/\phi z}\ell(x^{-1/\phi}) \quad \text{for } x \to \infty, \end{aligned} \tag{8}$$

where $x = \epsilon/t^{\phi}$. In systems where disorder plays the role of an irrelevant parameter, ϕ is positive, inhomogeneities only

affect the dynamics at early times, and $L(t)$ crosses over to the pure system behavior $L(t) \sim t^{1/z}$ at large times [11]. This usually happens if there is an upper limit for the height of energetic barriers. In contrast, when barriers of any size can be encountered, as in the fractal models considered in this paper and elsewhere, ϕ is negative and Eq. (8) describes the crossover from the early stage power law

$$L(t) \sim t^{1/z}, \tag{9}$$

with a temperature-independent growth exponent z, to the asymptotic form $L(t) = \lambda(\epsilon)\ell(t/\epsilon^{1/\phi})$ at the crossover length $\lambda = \epsilon^{1/(\phi z)}$. The functions $\lambda(\epsilon)$ and $\ell(t/\epsilon^{1/\phi})$ are in general hard to determine both analytically and numerically. However, some prediction can be made in the case of coarsening on deterministic fractal structures, as will be discussed in Sec. III.

A. Autocorrelation function

In order to discuss the effect of inhomogeneities on the form of the correlation functions, let us consider as a paradigm the autocorrelation function $C(t,t_w) = \mathcal{G}(r = 0; t, t_w)$. Generalizing the crossover approach (7) to this two-time quantity, one would expect the form

$$C(t,t_w;\epsilon) = \widehat{C}\left[\frac{L(t)}{L(t_w)}, \frac{\lambda(\epsilon)}{L(t_w)}\right], \tag{10}$$

where $\widehat{C}$ is a scaling function. In the context of disordered ferromagnetic systems, a superuniversality conjecture was proposed according to which the effect of disorder is simply accounted for by the slower growth of $L(t)$, while scaling functions entering correlation functions remain unchanged with respect to the clean case. This amounts to saying that, e.g. for the autocorrelation function, $\widehat{C}(x,y)$ should not depend on the second entry. The superuniversality property was checked in several models, arriving at different conclusions. Indeed, while $d = 1$ results [6,9] clearly demonstrate the absence of superuniversality, in the cases with $d \geqslant 2$, there is evidence both in favor [16,20,21] and against [6,11] its validity and there is presently an intense debate on the subject.

The original formulation of superuniversality was conceived for systems where inhomogeneities are introduced by disorder. The problem of determining the relevance of inhomogeneities in the scaling functions, however, may be posed on more general grounds and the simple systems studied in this paper may help the clarification of this issue.

III. COARSENING ON FRACTAL STRUCTURES

We will consider in the following the Ising model defined by the Hamiltonian

$$H[\sigma] = -J \sum_{\langle ij \rangle} \sigma_i \sigma_j, \tag{11}$$

where $\sigma_i = \pm 1$ is a unitary spin and $\langle ij \rangle$ are nearest neighbors on a graph. The dynamics is introduced by randomly choosing a single spin and updating it with a transition rate that in the numerical simulations will be chosen in the Metropolis form

$$w([\sigma] \to [\sigma']) = \min\{1, \exp(-\Delta E/k_B T)\}. \tag{12}$$

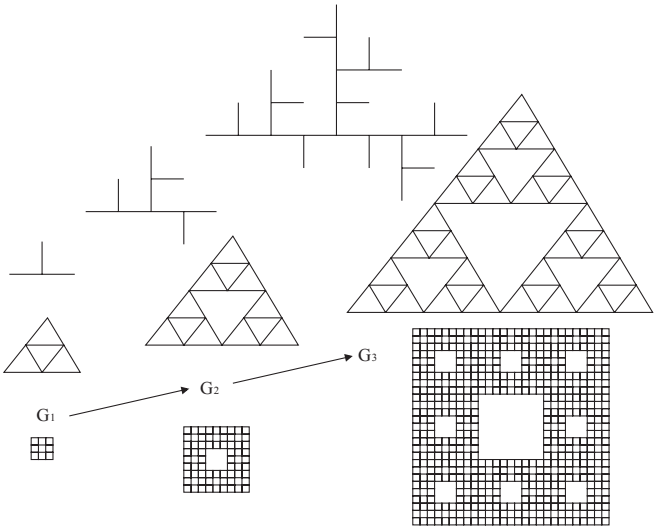

FIG. 1. Construction of the first three generations of the TF (top), SG (middle), and SC (bottom).

Here $[\sigma]$ and $[\sigma']$ are the spin configurations before and after the move and $\Delta E = H[\sigma'] - H[\sigma]$. Phase ordering is observed after a quench from an high initial temperature (assumed to be infinite in the following) to $T = 0$ or to a temperature below the critical one T_c. In order to infer the properties and the physical content of the quantities introduced in the preceding section, let us focus on the structures of the SG, the TF, and the SC [22,23], representing prototypical examples of finitely ramified (SG and TF) and infinitely ramified fractals (SC). Indeed, a wide class of fractal structures feature topological properties similar to the SG, TF, and SC [24]. In finitely ramified fractals, an arbitrary large part of the structure can be disconnected by removing a finite number of cutting bonds. In general, they admit an ordered phase only at $T = 0$. In a broad sense these structures can be considered as nontrivial topological analogs of a low-dimensional homogeneous system with $d \leqslant d_\ell$, d_ℓ being the lower critical dimension. Infinitely ramified graphs, in contrast, can possess a low-temperature ordered phase below a critical temperature T_c. All these fractals can be built starting from an elementary object, denoted by the first generation G_1, obtaining then an object of generation G_2 by combining G_1 parts, and then proceeding recursively as sketched in Fig. 1. In doing that, the linear size L_n of the structure at generation n grows as $L_n = f L_{n-1}$, where f is a constant that depends on the structure considered and, specifically, $f = 2$ for the SG and TF and $f = 3$ for the SC.

Since the Ising model on finitely ramified fractals is characterized by $T_c = 0$, phase ordering could in principle be truly asymptotic only after a quench to $T = 0$, where, however, the dynamics is frozen because activated moves are prevented. Nevertheless, as explained in Ref. [18], a preasymptotic coarsening stage of diverging duration is observed for sufficiently low temperatures, similarly to what happens, for instance, on the one-dimensional lattice. We will focus on this stage of the dynamics to study coarsening on finitely ramified structures.

During the evolution, energetic barriers arise due to the mechanism sketched in Fig. 2. Let us consider the SG first, represented in the top panel. The figure shows schematically

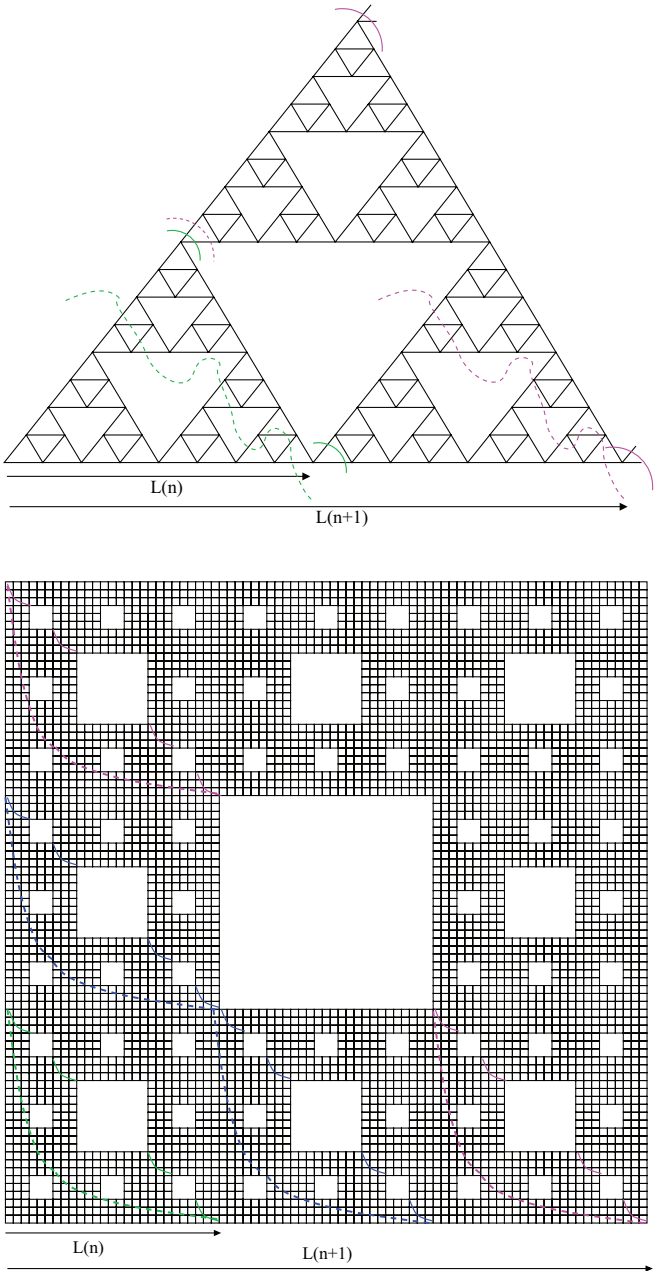

FIG. 2. (Color online) Schematic description of energy barriers in the SG (top) and SC (bottom). For the SG, the green and the magenta arches represent the positions of the interfaces in a configuration of minimum energy after a region of generation n (and $n+1$) has been reversed. The dashed green and magenta lines represent the configurations of the interface with larger energy while reversing the structure of generation n (and $n+1$). For the SC, the continuous green, blue, and magenta lines represent the positions of minimum energy of an interface after the reversal of part of the structure of generation n (and $n+1$). The corresponding dashed lines are the positions of larger energy to be exceeded.

the evolution of an interface that progressively spans a part of the structure. Initially, the position of the domain wall is outside the structure represented in the figure, in the left corner. This means that all the spins are, say, down. As time goes on, the interface enters the graph by moving across the intermediate position $I_n^{(\max)}$ indicated by a dotted green line (this means that spins on the left of the green line have been reversed upward). The index n refers to the fact that the interface is currently spanning the nth generation of the fractal. When the spins of the whole generation n have been reversed, the interface, depicted by two green arches, is located in the configuration $I_n^{(\min)}$ on the four cutting bonds. Since the energy of a domain wall is J times its length, it is clear that in $I_n^{(\min)}$ the interface has a minimum energy $E_n^{(\min)}$. On a finitely ramified structure, since the number of cutting bonds is finite, this quantity is bounded from above and for large n it becomes n independent, i.e., $E_n^{(\min)} = E^{(\min)}$. For the SG, $E^{(\min)} = 4J$ for any n since there are four cutting bonds for the interface, independently of n. Let us assume that the highest energy $E_n^{(\max)}$ of the system during the above process was reached in the (generic) configuration $I_n^{(\max)}$, so a barrier of height $\mathcal{E}_n = E_n^{(\max)} - E_n^{(\min)}$ has been crossed. Now the interface must proceed again to the right in order to reverse all the spins of the next generation $n+1$, thus reaching the position $I_{n+1}^{(\min)}$ located on the other four cutting bonds and indicated by the couple of magenta arches (all the spins in the figure at this stage have then been reversed). Also, this configuration has an energy equal to $E^{(\min)}$. The topology of the finitely ramified graph allows the system to attain this configuration by sequentially reversing parts of generation n of the structure. For instance, in the Sierpinski gasket, by first reversing another triangle of generation n, say, the bottom-right one in Fig. 2. This event is analogous to the one described before. In particular, the interface in the intermediate position $I_{n+1}^{(\max)}$, depicted by a dashed magenta line, is analogous to the previous one at $I_n^{(\max)}$ (dotted green arch), except for the presence of an extra part around certain cutting bonds, which, in the present example, are indicated by a dashed magenta arch. For low temperatures the number of these cutting bonds tends to be minimized and it does not depend on the generation. Denoting by $E_{n+1}^{(\max)}$ the maximum energy reached by the system in the reversal of the $n+1$ generation, one concludes that $E_{n+1}^{(\max)} = E_n^{(\max)} + E_c$, where E_c is the amount of extra energy due to the new part of interface (the dotted magenta arch in the figure). Writing $E_c = Jn_c$, where n_c is double the number of broken bonds associated with the energy E_c, for the SG, one has $n_c = 4$. We recall that in general n_c does not depend on n. Then

$$\mathcal{E}_{n+1} \simeq \mathcal{E}_n + Jn_c \tag{13}$$

or, equivalently, rewriting $\mathcal{E}$ in terms of the size L_n of the nth generation,

$$\mathcal{E}(fL_n) \simeq \mathcal{E}(L_n) + Jn_c. \tag{14}$$

From this relation, dropping the index n, one has

$$\mathcal{E} \simeq \frac{Jn_c}{\ln f} \ln L. \tag{15}$$

Inserting this form into the Arrhenius relation (3), we arrive at an algebraic growth law as in Eq. (5) with

$$\zeta \simeq a \frac{J}{T} \tag{16}$$

and

$$a \simeq \frac{n_c}{k_B \ln f} \tag{17}$$

at low temperatures. The argument has been developed by referring to the deterministic SG, but it is expected to hold also for the TF (with $n_c = 2$) and in general for finitely ramified deterministic and disordered structures, as for all of them an arbitrary large part can be disconnected by cutting a finite number of links.

A similar argument applies to infinitely ramified structures and it will be schematically illustrated for the SC with the help of the lower panel of Fig. 2. As for the SG, an interface enters the portion of the fractal considered from, say, the bottom-left edge, crossing a region of generation n, passing through a high-energy position depicted as an arch-shaped dashed green line. The evolution then proceeds towards the position $I_n^{(\min)}$, which in the figure is depicted by a continuous green line that roughly spans the diagonal of the nth generation. Here the energy reaches a minimum $E_n^{(\min)}$ because the largest hole available at generation n is crossed, thus minimizing the number of misaligned spins. Then the domain wall moves to the next high-energy configuration, depicted as a couple of dashed arch-shaped blue lines, and then to the minimum energy position $I_{n+1}^{(\min)}$ depicted by a continuous diagonal blue line. Eventually the magenta configurations are progressively reached by the interface. Notice that these configurations have the same energy as the blue ones. It is clear from the figure that the energies of the blue (or magenta) configurations occupied at generation $n+1$ are double those of the green ones at generation n. Hence one can write, in place of (14),

$$\mathcal{E}(fL_n) = u\mathcal{E}(L_n), \tag{18}$$

where $u = 2$ for the SC. Hence, in place of Eq. (15) we find

$$\mathcal{E}(L_n) \simeq bJL_n^{d_{fl}}, \tag{19}$$

where $d_{fl} = \ln u/\ln f$ is in general the fractal dimension of the intersection of the fractal structure with a line, that is, the border of the interface, corresponding to the cut set (e.g., it is $d_{fl} = \ln 2/\ln 3$ for the SC considered in the figure), and from Eq. (3) we arrive at Eq. (2), with

$$\psi = d_{fl}. \tag{20}$$

This argument, developed for the SC, is expected again to be of general validity for all infinitely ramified structures.

In conclusion, according to the above discussion, finitely (SG and TF) and infinitely (SC) ramified fractals represent typical examples where barriers increase logarithmically and algebraically with L [Eqs. (4) and (6), respectively] due to their topological properties. Correspondingly, the growth law is expected to be a power law (with a temperature-dependent exponent) or a logarithmic behavior [Eqs. (5) and (2), respectively]. These behaviors should be observed when the energy scale k_BT associated with temperature fluctuations is small with respect to the height $\mathcal{E}$ of the barriers. Conversely, for $\mathcal{E} \ll k_BT$, the effect of the barriers is negligible. Interfaces diffuse freely in this case and, in analogy to what is observed on regular lattices, one expects to observe a power-law behavior as in Eq. (9), characterized by the temperature-independent exponent that describes the displacement $\langle x^2\rangle \propto t^{1/z}$ of a random walker on the structure. For a fractal graph having spectral and fractal dimensions d_s and d_f, respectively, it is $z = 2d_f/d_s$ [25]. We remark that this same power law is predicted by approximate theories [26] to be the correct asymptotic growth law, whereas our arguments indicate that it can only be preasymptotic.

All these behaviors can be fitted into the crossover scenario described by Eq. (7) provided $z = d_s/2d_f$ and

$$\begin{aligned} &\ell(x) \propto x^{1/\zeta} \quad \text{for finitely ramified graphs} \\ &\ell(x) \propto (\ln x)^{1/\psi} \quad \text{for infinitely ramified graphs,} \end{aligned} \tag{21}$$

with ζ and ψ given in Eqs. (16) and (20). The crossover length λ is given by the condition

$$\mathcal{E}(\lambda) \simeq k_BT. \tag{22}$$

Using Eqs. (15) and (19), this implies that

$$\begin{aligned} &\lambda \sim \exp(k_BT \ln f/Jn_c) \quad \text{for finitely ramified graphs} \\ &\lambda \sim (k_BT/J)^{1/d_{fl}} \quad \text{for infinitely ramified graphs.} \end{aligned} \tag{23}$$

IV. NUMERICAL SIMULATIONS

In this section we present the results of numerical simulations of the dynamics of the Ising model after a quench on the SG, the TF, and the SC. In the simulations we will consider systems with $n = 9$, 8, and 6 generations, respectively. With these choices finite-size effects are not observed in the range of times considered. The system is prepared in a completely disordered state where spins are set to $\sigma_i = \pm 1$ randomly and independently on each site i, corresponding to an infinite-temperature equilibrium initial state. The evolution is then implemented by flipping randomly chosen single spins with the Metropolis rate (12), where T is the temperature at its quench value. We always set $k_B = 1$ and $J = 1$ or, stated differently, we measure temperature in units of J/k_B. We consider a modified dynamics called no-bulk-flip dynamics, where spins that are aligned with all the nearest neighbors, namely, in the bulk of an ordered domain, cannot flip. It was shown that this dynamics, which has been tested and used in a number of studies [18,27], does not change the large-scale properties of the system and improves the speed of the simulation and the quality of the results. In order to grasp at least the basic physics inspiring the no-bulk-flip rule let us recall that in a coarsening system all the large-scale and long-time properties are uniquely determined by the motion of the ordered domains walls. Well inside the domains, regions of spins correlated over a length $\xi(T)$ can rapidly change sign over a characteristic time $\xi(T)^z$, where z is the dynamical exponent. However, since for large times t and $T < T_c$, $\xi(T)$ is always negligible with respect to $L(t)$, the flipping of these thermal islands affects only small-distance and short-time properties, which are not the universal ones we are interested in. Further details on this accelerated dynamics can be found in Refs. [17,27]. For the SG, we study quenches to different final temperatures in the range $T \in [0.8 - 3.4]$. For $T > 3.4$ the system very rapidly reaches the disordered equilibrium state and the coarsening stage cannot be observed. In contrast, for $T < 0.8$ the dynamics becomes exceedingly slow to obtain reliable results with our computational resources. Similarly, for the TF we consider quenches in the range of final temperatures $T \in [0.2 - 3]$ and for the SC $T \in [1 - 3]$.

On a homogeneous structure, assuming scaling (1), the equal-time correlation function

$$G(r;t) = \langle \sigma_i(t)\sigma_j(t)\rangle \tag{24}$$

depends only on the distance r between i and j. From this the typical length $L(t)$ is usually extracted, e.g., as the half height width $G(r = L(t);t) = 1/2$. Although on a generic graph the notion of distance is not straightforward, one can reduce its definition to the usual one along certain directions, as done in Refs. [18,19]. Proceeding analogously, here we arrive at a determination of $L(t)$. This quantity is shown in Fig. 3 for quenches to different final temperatures.

A first trivial observation is that in the structures considered in the simulations there is a lower cutoff $L_{\rm hole}$ of the size of the holes. Hence, for $L(t) < L_{\rm hole}$ the fractal nature of the graph is not revealed and we expect to observe the same behavior as on a homogeneous lattice. Here $L_{\rm hole}$ is of the order of the size of the first generation and, in the cases considered here, $L_{\rm hole} \simeq 3$. Very early data with $L(t) < L_{\rm hole}$, therefore, do not describe the effect of the fractal structure and we will restrict the discussion to only $L(t) > L_{\rm hole}$.

For all structures considered here, one sees very clearly a crossover from an early regime $L(t) \ll \lambda$, where curves for different temperatures roughly collapse, to a late stage with a strongly-temperature-dependent behavior. This is what one would expect from the picture described in the preceding sections. According to the discussion of Sec. III, if such a crossover is described by Eq. (7), a number of predictions can be done, which we will check in the following.

A. Crossover length

We start from the behavior of the crossover length λ given in Eq. (23). For the SG, using $f = 2$ and $n_c = 4$ one has $\ln f/Jn_c \simeq 0.17$. Using Eq. (23) one concludes that, in the range of temperatures explored ($T \in [0.8 - 3.4]$), λ can be varied at most by a factor 1.57. In Fig. 3 (top-left panel) we have indicated by a dashed horizontal line the value of λ obtained from Eq. (23) by adjusting the proportionality constant in such a way that for $L(t) > \lambda$ only the asymptotic power-law growth (21) (with $\zeta \neq z$) is observed. This can be done rather precisely for the lowest temperatures. Since λ can be varied only by the small factor 1.57, it is clear that even for the highest temperature one cannot obtain a significative range $L_{\rm hole} < L(t) < \lambda$ to clearly determine the preasymptotic stage, where Eq. (9) should hold with a temperature-independent exponent $z = 2d_f/d_s$ (this law is represented by the dashed magenta line). Notice that at the highest temperatures $L(t)$ grows approximately as in Eq. (9) but, as will be discussed below, for the different reason that the asymptotic temperature-dependent exponent ζ approaches the value $z = 2d_f/d_s$ at high temperatures. A similar situation is found for the TF (top-right panel). Here the smaller value of n_c ($n_c = 2$) allows λ to vary by a slightly larger factor, i.e., 2.46. On this structure, then, at variance with the SG, one should be able to detect the preasymptotic regime $L_{\rm hole} < L(t) < \lambda$ at least for the larger temperatures.

For the SC we have plotted in Fig. 3 (bottom panels) the crossover length λ obtained from Eq. (23) by using $d_{fl} = \ln 2/\ln 3$ and adjusting the proportionality constant in such a way that the crossover from an early power law to asymptotic logarithmic behavior occurs around λ. As shown in Fig. 3, our estimate of λ fits quite nicely at a semiquantitative level with the data.

B. Early stage

Next let us consider the first regime for $L(t) \ll \lambda$ that should obey the power-law behavior (9) with the temperature-independent exponent $z = 2d_f/d_s$. As already discussed above, this preasymptotic regime is too short to be studied in the SG. For the TF this should in principle be observed at least at the largest temperature $T = 2.5$. However, as can be seen in Fig. 3, the crossover appears to be very broad, preventing clear-cut evidence of the preasymptotic behavior also in this structure.

On the contrary, for the SC at the highest quench temperature $T = 3$ this stage lasts for more than a decade. Here one observes the expected power law with exponent $z = 2d_f/d_s$ (such a law is represented by the dashed magenta line). This shows that, indeed, in a preasymptotic regime barriers do not play a relevant role and interfaces perform a random walk on the graph. Notice also that, as already observed in Refs. [18,19], an oscillatory behavior is superimposed on a globally increasing trend. This feature is observed in all the dynamical regimes and also in the SG and TF. Although the very limited extent of time that can be reached in simulations does not allow one to observe more than at most one to two oscillations, thus preventing any precise analysis, a semiquantitative inspection of the data clearly suggests that these might be log-time periodic. This periodicity is observed in a number of apparently different phenomena, ranging from fracturing of heterogeneous solids [28] to stock market indexes [29] and from magnetic systems with a lack of translational symmetry [30] to phase-separating fluids under shear [31]. This feature is generally associated with the presence of a discrete scale invariance [32], which in the present case induces a recurrent trapping of the interfaces when a complete generation of the fractal has been ordered. The presence of such log-periodic oscillations has been analytically proven for a random walker diffusing on these fractal structures [33].

C. Late stage

The next step is the determination of the asymptotic growth law, namely, the function ℓ, which should behave as in Eq. (21). For the SG and the TF it is clear that the curves oscillate around a net power-law behavior, as already observed in Ref. [18]. This is what was expected for finitely ramified graphs, according to Eq. (21). Our arguments provide the prediction (16) and (17) for the low-temperature behavior of ζ. In order to check this we have plotted $1/\zeta$ against temperature in the inset of the top panels of Fig. 3. For low T the data show good agreement with the expected behavior, which is represented by the dashed blue lines. Notice that, in this case, there are no fitting parameters since also the value of the constant a has been inferred.

In the case of the SC, the logarithmic growth of $L(t)$ forces one to reach much longer times, particularly at low temperatures, and this in turn increases the computational

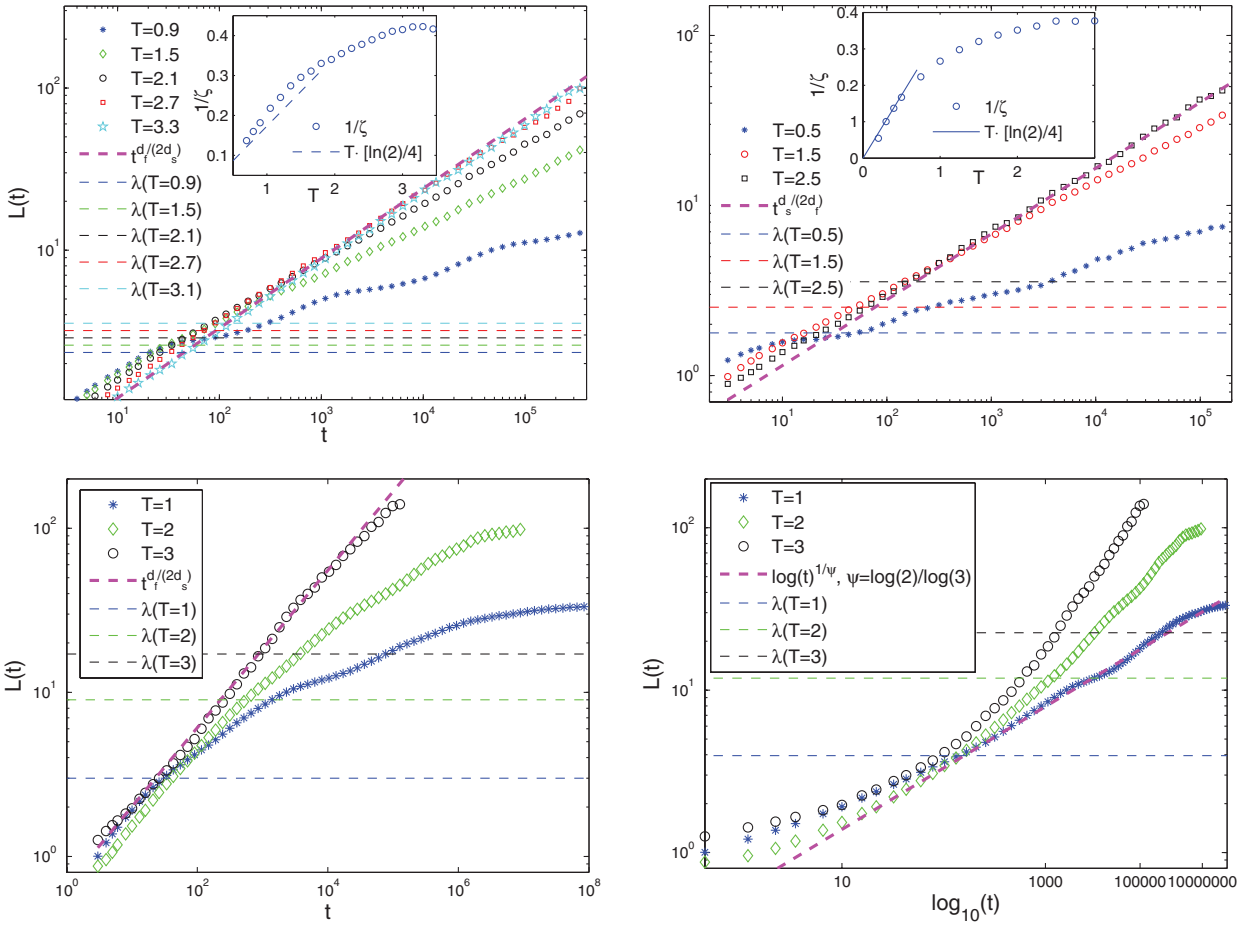

FIG. 3. (Color online) Typical size $L(t)$ (symbols) plotted against time on a log-log plot for an Ising model quenched to different final temperatures (see legend) on the SG (top-left panel), the TF (top-right panel), and the SC (bottom panels). The bold dashed magenta line in the top- and bottom-left panels is the expected short-time behavior $L(t) \sim t^{1/z}$, with $z = 2d_f/d_s$, while in the bottom-right panel it represents the asymptotic logarithmic law $L(t) \sim (\ln t)^{1/\psi}$, with $\psi = d_{fl} = \ln 2/\ln 3$. The horizontal dashed lines represent the crossover length λ. In the inset of the top panels the exponent $1/\zeta$, obtained from the data of the main part of the figure, is plotted against T. The dashed blue line is the prediction (16) and (17).

effort limiting the possibility of a large statistics over many realizations of the thermal histories. Moreover, the screening due to the oscillations is more severe. Nevertheless, the data of the top-right panel of Fig. 3 show quite unambiguously a crossover to a slower growth law around $L(t) \simeq \lambda$. According to our general picture, this should be described by the logarithmic form of Eq. (21). In order to check this we have plotted in the bottom-left panel the same data but with an extra logarithm on the time axis. In this plot the form of Eq. (21) is a straight line with slope $1/\psi$. This is consistent with our data for $L(t) > \lambda$. The numerical results show that the exponent ψ decreases when T is increased. In the limit of low temperature, the value of Eq. (20) is predicted. The corresponding law is represented by a dashed magenta line in the bottom-left panel of Fig. 3. Here one observes very nice agreement with the data for the lowest temperature ($T = 1$), suggesting the correctness of our argument.

D. Autocorrelation function

Finally, our simulations allow us to comment on the role of the inhomogeneities in the scaling functions of correlation functions. We will consider in the following the autocorrelation function

$$C(t,t_w) = \frac{1}{N}\sum_{i=1}^{N}\langle \sigma_i(t)\sigma_i(t_w)\rangle, \tag{25}$$

where N is the number of spins in the structure, for which the scaling form (10) is expected.

As discussed previously, because of the smallness of λ on the SG and the broad form of the scaling functions in the TF, the whole crossover pattern can be better detected in the SC. Hence we concentrate on this structure in the following. In Fig. 4 we plot the autocorrelation function measured after different waiting times t_w. The top panel refers to the quench to the highest temperature $T = 3$, where, according to the data of Fig. 3, one can access both the preasymptotic regime and the crossover to the late stage and the role of the second entry of the scaling function in Eq. (10) can be studied. Interestingly, the crossover phenomenon is fully displayed in the figure. Indeed, the two curves for the shortest waiting times ($t_w = 10$ and 20) almost collapse. The small residual dependence on t_w, namely, the fact that the collapse is not perfect, is probably due

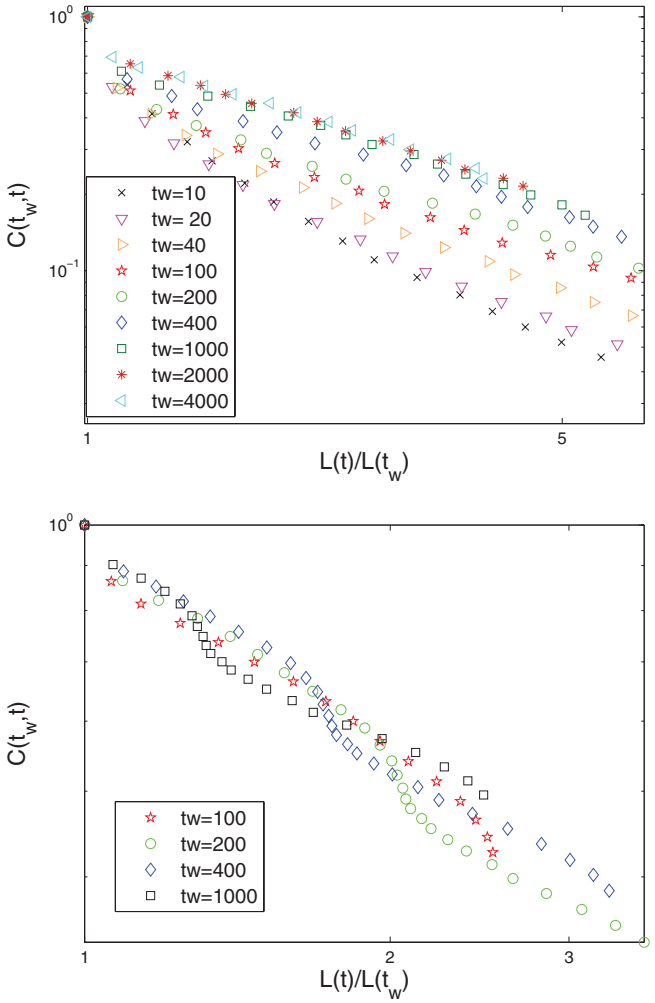

FIG. 4. (Color online) Autocorrelation function $C(t,t_w)$ plotted against $L(t)/L(t_w)$ for different values (see legend) of t_w. In the top panel a quench to $T = 3$ is considered, while in the bottom it is $T = 1$.

to the fact that the presence of the crossover is already slightly felt even at these early times [but we cannot reduce t_w further because of the constraint $L(t_w) > L_{\rm hole}$]. However, the picture shows that the separation between these two curves is much smaller than the one between the following ones, which clearly indicates a convergence of the data to a limiting master curve for $L(t_w) \ll \lambda$. In view of Eq. (10) this means that the second entry $\lambda/L(t_w)$ is so large that $\widehat{C}[L(t)/L(t_w),\lambda(T)/L(t_w)] \simeq \widehat{C}[L(t)/L(t_w),\infty]$. Then, upon increasing $L(t_w)$, the second argument of $\widehat{C}$ decreases and becomes relevant. Indeed, the collapse is lost and there is a clear tendency of the curves to move to larger values, as already noticed in Ref. [18]. This signals the crossover from the early stage to the late regime. Finally, for larger values of $L(t_w)$ [$L(t_w) \gg \lambda$] one has again a tendency to collapse on a master curve that corresponds to $\widehat{C}[L(t)/L(t_w),0]$. This is verified for $t_w = 1000,2000,4000$.

In order to complete the analysis we consider also the quench to the lower temperature $T = 1$. In this case, since λ is smaller, the limiting curve $\widehat{C}[L(t)/L(t_w),0]$ should be achieved at earlier t_w. Our results are plotted in the bottom panel of Fig. 4. At this low temperature the autocorrelation function is strongly oscillating. This is the counterpart of the periodic modulations already observed in the growth law. These oscillations hinder somehow the collapse of the curves. Nevertheless, one observes that already from such short waiting times as $t_w = 100$ onward the curves do not show any tendency to move upward, at variance with the case with $T = 3$. This can be interpreted as due to the fact that since λ is much smaller at $T = 1$, the collapse on the master curve $\widehat{C}[L(t)/L(t_w),0]$ is already achieved at these early times. Clearly, since λ is small, the precrossover collapse on $\widehat{C}[L(t)/L(t_w),\infty]$ is not observed here. Notice that the two master curves $\widehat{C}[L(t)/L(t_w),\infty]$ and $\widehat{C}[L(t)/L(t_w),0]$ in the top panel are very well separated, clearly indicating the relevance of the second entry in the scaling function of Eq. (10). The whole behavior of C, which is captured by the two-parameter scaling (10), shows unambiguously the relevance of the inhomogeneities, entering through the length λ, in determining the shape of the scaling functions.

V. CONCLUSION

In this paper we have studied the phase-ordering kinetic of a ferromagnetic system with a scalar order parameter on fractal graphs. We have proposed a scaling approach, inspired by renormalization-group ideas, where a crossover between distinct dynamical behaviors is induced by the presence of a length λ introduced by the topological properties of the graph. The transition between the early and asymptotic stages is observed when the typical size $L(t)$ of the growing ordered domains reaches the crossover length λ. In this general framework, two classes of inhomogeneous substrates can be defined according to the nature of the activated processes that set in during the evolution. Specifically, we argue that on finitely ramified graphs the free-energy barriers encountered by domains walls grow logarithmically with $L(t)$, whereas they increase as a power law on all the other structures. This produces different asymptotic growth laws (power laws vs logarithmic) and a different dependence of the crossover length λ on the model parameters. We have tested these ideas by numerical simulations of the Ising model on two model structures where, due to their relative simplicity, one can exhibit explicit predictions for the behavior of $L(t)$ and λ, which conform very well to the numerical data.

The models studied in this paper can be considered as simple prototypical systems to understand the more general and still open problem of phase ordering in inhomogeneous systems. A natural question is then if (and how) the results of this article can be extended to more general situations. For instance, one might wonder if a similar picture holds in systems where dilution is random instead of being, as in this paper, deterministic. Following the arguments developed in Secs. II and III, one realizes that neither the deterministic character nor the fractal nature is really determinant. Instead, the fundamental ingredient is whether the position of minimum energy of interfaces contains a number n_c of broken bonds that is independent of $L(t)$ or if such a number scales with (some power of) $L(t)$. This in turn is related to fact that the corresponding graph does not sustain a ferromagnetic phase ($T_c = 0$) or it does ($T_c > 0$), respectively. Extending this argument to the case of random dilution, we can predict

an asymptotic logarithmic growth law as in Eq. (2) for the randomly diluted (bond or site) Ising model with a fraction of occupied sites (or bonds) $p > p_c$, where p_c is the percolation threshold. Right at $p = p_c$, in contrast, we expect a power-law growth as in Eq. (5). Notice that, at variance with the fractal models studied in this article, for randomly diluted systems one can tune continuously the parameter p that controls the closeness to the threshold case $p = p_c$. Finally, it would be interesting to understand if similar concepts can be extended to interpret a different system where the inhomogeneous character is not due to dilution but to other agents such as random coupling constants or spatially varying external fields.

[1] A. J. Bray, Adv. Phys. **43**, 357 (1994).

[2] For reviews, see F. Corberi, L. F. Cugliandolo, and H. Yoshino, in *Dynamical Heterogeneities in Glasses, Colloids, and Granular Media*, edited by L. Berthier, G. Biroli, J.-P. Bouchaud, L. Cipeletti, and W. van Saarloos (Oxford University Press, Oxford, 2010); J. P. Bouchaud, L. F. Cugliandolo, J. Kurchan, and M. Mezard, in *Spin Glasses and Random Fields*, edited by A. P. Young (World Scientific, Singapore, 1997); L. F. Cugliandolo, in *Slow Relaxation and Non-Equilibrium Dynamics in Condensed Matter*, edited by J. L. Barrat, J. Dalibard, J. Kurchan, and M. V. Feigelman (Springer, Heidelberg, 2002).

[3] S. Puri, Phase Transit. **77**, 469 (2004).

[4] M. Henkel and M. Pleimling, Europhys. Lett. **76**, 561 (2006).

[5] M. Henkel and M. Pleimling, Phys. Rev. B **78**, 224419 (2008).

[6] E. Lippiello, A. Mukherjee, S. Puri, and M. Zannetti, Europhys. Lett. **90**, 46006 (2010).

[7] H. Park and M. Pleimling, Phys. Rev. B **82**, 144406 (2010).

[8] Z. W. Lai, G. F. Mazenko, and O. T. Valls, Phys. Rev. B **37**, 9481 (1988); K. Tafa, S. Puri, and D. Kumar, Phys. Rev. E **63**, 046115 (2001).

[9] F. Corberi, A. de Candia, E. Lippiello, and M. Zannetti, Phys. Rev. E **65**, 046114 (2002).

[10] D. S. Fisher and D. A. Huse, Phys. Rev. B **38**, 373 (1988); L. F. Cugliandolo, Physica A **389**, 4360 (2010).

[11] F. Corberi, E. Lippiello, A. Mukherjee, S. Puri, and M. Zannetti, Phys. Rev. E **85**, 021141 (2012).

[12] R. Burioni and D. Cassi, J. Phys. A **38**, R45 (2005).

[13] H. Furukawa, J. Phys. Soc. Jpn. **58**, 216 (1989); Phys. Rev. B **40**, 2341 (1989); M. Zannetti, in *Kinetics of Phase Transitions*, edited by S. Puri and V. Wadhawan, (CRC, Boca Raton, FL, 2009), p. 153.

[14] S. J. Cornell, K. Kaski, and R. B. Stinchcombe, Phys. Rev. B **44**, 12263 (1991); F. Corberi, C. Castellano, E. Lippiello, and M. Zannetti, Phys. Rev. E **65**, 066114 (2002).

[15] S. Puri and N. Parekh, J. Phys. A **26**, 2777 (1993); E. Oguz, A. Chakrabarti, R. Toral, and J. D. Gunton, Phys. Rev. B **42**, 704 (1990); E. Oguz, J. Phys. A **27**, 2985 (1994).

[16] M. Rao and A. Chakrabarti, Phys. Rev. Lett. **71**, 3501 (1993); C. Aron, C. Chamon, L. F. Cugliandolo, and M. Picco, J. Stat. Mech. (2008) P05016.

[17] F. Corberi, E. Lippiello, A. Mukherjee, S. Puri, and M. Zannetti, J. Stat. Mech. (2011) P03016.

[18] R. Burioni, D. Cassi, F. Corberi, and A. Vezzani, Phys. Rev. E **75**, 011113 (2007).

[19] R. Burioni, F. Corberi, and A. Vezzani, J. Stat. Mech. (2009) P02040.

[20] R. Paul, S. Puri, and H. Rieger, Europhys. Lett. **68**, 881 (2004); Phys. Rev. E **71**, 061109 (2005).

[21] S. Puri, D. Chowdhury, and N. Parekh, J. Phys. A **24**, L1087 (1991); S. Puri and N. Parekh, *ibid.* **25**, 4127 (1992); A. J. Bray and K. Humayun, *ibid.* **24**, L1185 (1991); A. Sicilia, J. J. Arenzon, A. J. Bray, and L. F. Cugliandolo, Europhys. Lett. **82**, 1001 (2008).

[22] Y. Gefen, A. Aharony, Y. Shapir, and B. B. Mandelbrot, J. Phys. A **16**, 435 (1983); **17**, 1277 (1984).

[23] R. Burioni, D. Cassi, F. Corberi, and A. Vezzani, Phys. Rev. Lett. **96**, 235701 (2006).

[24] R. Rammal, Phys. Rev. B **28**, 4871 (1983); Y. Lin, B. Wu, and Z. Zhang, Phys. Rev. E **82**, 031140 (2010); P. Buonsante, R. Burioni, and A. Vezzani, *ibid.* **84**, 021105 (2011).

[25] J. P. Bouchaud and A. Georges, Phys. Rep. **195**, 127 (1990).

[26] U. Marini Bettolo Marconi, Phys. Rev. E **57**, 1290 (1998).

[27] F. Corberi, E. Lippiello, and M. Zannetti, Phys. Rev. E **63**, 061506 (2001); Eur. Phys. J. B **24**, 359 (2001); Phys. Rev. E **68**, 046131 (2003); **72**, 056103 (2005); **78**, 011109 (2008); E. Lippiello, F. Corberi, A. Sarracino, and M. Zannetti, *ibid.* **78**, 041120 (2008); F. Corberi and L. F. Cugliandolo, J. Stat. Mech. (2009) P05010.

[28] R. C. Ball and R. Blumenfeld, Phys. Rev. Lett. **65**, 1784 (1990); M. Sahimi and S. Arbabi, *ibid.* **77**, 3689 (1996); D. Sornette, Phys. Rep. **297**, 239 (1998).

[29] D. Sornette and A. Johansen, Quant. Finance **1**, 452 (2001); Eur. Phys. J. B **17**, 319 (2000); Physica A **245**, 411 (1997).

[30] R. F. S. Andrade, Phys. Rev. E **61**, 7196 (2000).

[31] F. Corberi, G. Gonnella, and A. Lamura, Phys. Rev. E **62**, 8064 (2000); **61**, 6621 (2000); Phys. Rev. Lett. **83**, 4057 (1999); **81**, 3852 (1998); A. Lamura, G. Gonnella, and F. Corberi, Eur. Phys. J. B **24**, 251 (2001).

[32] D. Sornette, *Chaos, Fractals, Self-Organization and Disorder: Concepts and Tools* (Springer, Berlin, 2004).

[33] P. J. Grabner and W. Woess, Stoch. Proc. Appl. **69**, 127 (1997).